Improved Pose Detection for Single Camera Real-Time MR Motion Correction Using a Self-Encoded Marker

C. Forman[1], M. Aksoy[2], M. Straka[2], J. Hornegger[1], and R. Bammer[2]
[1]Pattern Recognition Lab, Department of Computer Science, Friedrich-Alexander-University Erlangen-Nuremberg, Erlangen, Germany, [2]Department of Radiology, Stanford University, Stanford, CA, United States

INTRODUCTION – Correcting patient motion in MRI is a challenge that is still not fully solved. Although many correction approaches have been suggested, a considerable limitation for the majority of them is that they are only working on a subset of pulse sequences. From a routine clinical imaging perspective this is insufficient. Recently, a new and more promising crop of motion correction methods has been suggested that relies on optical pose tracking, works prospectively, and is independent from the MR data acquisition process [1,2,3,4]. To avoid line-of-sight obstructions that can occur with external video tracking [1,2], Aksoy *et al*. [4] introduced an MR-compatible camera to track a planar checkerboard marker on the patient's forehead (Fig. 1a). One potential limitation of this approach is the limited field of view (FOV) of the camera due to the restricted space inside of the scanner bore and the lens distortions, which tend to increase peripherally. This restricts the amount of motion that can be reliably detected to a narrow range (±25mm) and also renders the approach sensitive to where the marker is placed within the FOV of the camera (Fig 1b, left). Clearly, this would limit acceptance of this approach in clinical routine. To overcome these restrictions, a self-encoded marker design (Fig. 1b, right) was developed and compared against the traditional checkerboard marker.

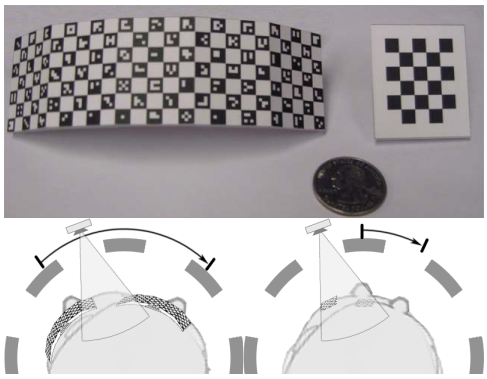

Figure 1: *(a)* Image of the self-encoded marker (left) and checkerboard marker (right). (b) The range of patient motion, that can be tracked is larger for the self-encoded marker compared to the planar marker..

MATERIALS and METHODS – (a) System Description: As described elsewhere [4], a camera is mounted on the 8 channel head coil to track a marker of known geometry, which allows one to determine its location in 3D. Here, the images of the camera are processed by an independent tracking processor, which sends – via a fast network connection – pose updates to the MR sequencer in real-time. The sequencer uses these incoming updates (at a ~30Hz rate) to adjust gradients and RF frequency and adapts slice orientation and location according to the patient's new position. The total system response time is ~50msec. **(b) Self-encoded Marker:** To overcome the aforementioned FOV limitation, a larger 3D-marker was developed which has each of the black quads of the checkerboard encoded by an additional unique and rotation invariant ID (Fig. 1c). These position encryptions are used by the tracking processor to identify the area of the marker that is currently within the FOV of the camera. This allows one to track motion by only looking at a subsection of a maker of larger dimension. It also allows one to restrict the aperture of the camera to keep only the part of the FOV with acceptable lens distortion and focusing. **(c) Accuracy Experiments:** First, accuracy and precision of both the checkerboard and self-encoded marker was compared outside the scanner using identical pre-described motion performed using a highly accurate 'pan-tilt unit'. In this experiment progressive yaw (30x2°) motion was separately conducted to each marker. This motion is similar to a patient's head rotation. **(d) In-vivo Experiments:** *In-vivo* experiments were performed using axial 3D SPGR scans (TR/TE 9.5ms/4.1ms, α=20°, matrix=192x192x96, FOV=24cm) with real-time pose feed from the tracking processor using either the checkerboard or the self-encoded marker. During scanning with either marker, the healthy volunteer was asked to rotate the head every 30 seconds. An additional scan without motion correction was obtained as reference.

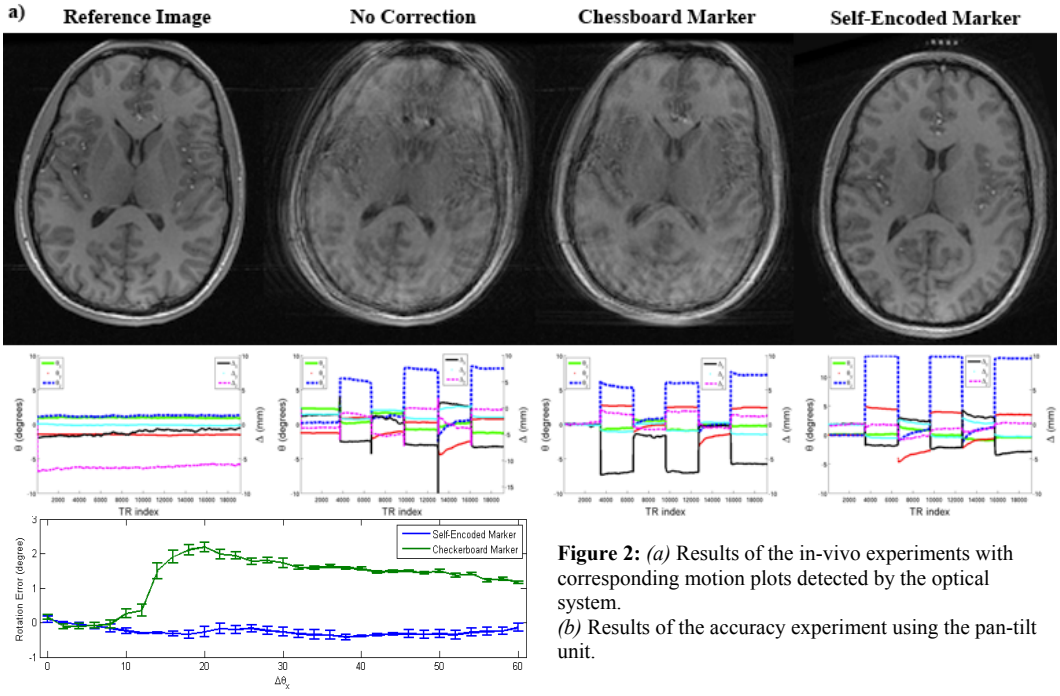

Figure 2: *(a)* Results of the in-vivo experiments with corresponding motion plots detected by the optical system.
(b) Results of the accuracy experiment using the pan-tilt unit.

RESULTS – For the accuracy experiment, the motion is measured relative to an initial first position of the marker. The error – defined as the difference between actual motions performed by the pan-tilt unit and motions detected by the tracking system – are shown in Figure 2a. It can be seen that the accuracy of the position estimates of the checkerboard marker dropped about 1.5-2° after a rotation > 14°. A remarkably better accuracy over a much wider range could be achieved for the self-encoded marker (Fig. 2a). Precision was below 0.1°. The resulting images from the *in-vivo* experiments are shown in Figure 2b. Due to the fact that part of the checkerboard marker would have otherwise been out of the FOV of the camera, the patient could only perform rotations within a range of 6°. Using the identical setup, the self-encoded marker was able to detect a rotation of the patient's head within a range of 13°. Without correcting for motion, the scan showed significant motion artifacts. Adaptive motion correcting, using the checkerboard marker, reduced these artifacts, but was unable to fully compensate them. Using the self-encoded marker, the adaptive motion-correction performed remarkable better and was able to successfully remove the majority of motion-induced errors despite the fact that the head rotations were over an increased range.

DISCUSSION – A new, self-encoded marker for mono-vision based pose tracking was introduced, which clearly offered advantages over a traditional checkerboard in terms of accuracy and precision over a much wider range of pose changes performed. In-vivo experiments were of great diagnostic quality and the system was essentially able to adapt for motion over the entire range possible within the head coil.

References [1] Dold et al., Acad. Radiol; 13:1093-1103, 2006 [2] Zaitsev et al., NeuroImage, 31:1038-1050, 2006. [3] Aksoy et al, ISMRM, 2008 [4] Aksoy et al, ISMRM, 2009 **Acknowledgements** This work was supported in part by the NIH (1R01EB008706, 5R01EB002711, 1R01EB006526, 1R21EB006860, P41RR09784), Lucas Foundation, Oak Foundation, and GE Healthcare.